



# Effect of a high magnetic field on the morphology and magnetic properties of the MnBi compound during the Mn<sub>1.08</sub>Bi–MnBi phase transformation process

Xi Li<sup>a,b,\*</sup>, Zhongming Ren<sup>a</sup>, Yves Fautrelle<sup>b</sup>, Kang Deng<sup>a</sup>

<sup>a</sup> Shanghai Key Laboratory of Modern Metallurgy & Materials Processing, Shanghai University, Shanghai 200072, PR China

<sup>b</sup> EPM-SIMAP, ENSHMG BP 38402 St. Martin d'Heres Cedex, France

## ARTICLE INFO

### Article history:

Received 27 September 2008

Received in revised form

23 February 2009

Available online 1 April 2009

### Keywords:

High magnetic field

Bi–Mn alloys

Magnetization

Microstructure

Magnetic force

## ABSTRACT

Effect of a 10 T high magnetic field on the morphology and magnetic properties of the MnBi compounds during the Mn<sub>1.08</sub>Bi–MnBi phase transformation has been investigated. Results indicate that the field has split the MnBi crystal along the (001)-crystal plane during the Mn<sub>1.08</sub>Bi–MnBi phase transformation process and the split MnBi crystals align and aggregate along the magnetic field direction. Along with the change of the MnBi phase morphology, the magnetic property changes greatly. Indeed, with the alignment and aggregation of the split MnBi phases, the saturation magnetization  $M_s$  and the magnetic susceptibility  $\chi$  increase, and the coercive field  $H_c$  and the remnant magnetization  $M_r$  decrease. This implies that a high magnetic field may have caused the magnetic property of the MnBi phase to transform towards soft magnetism. Above results may be attributed to the enhancement of the magnetization and the Mn<sub>1.08</sub>Bi–MnBi phase transformation in a high magnetic field.

© 2009 Elsevier B.V. All rights reserved.

## 1. Introduction

Recently, owing to the development in the superconducting magnets, a high magnetic field up to 12 T has been widely used to improve material properties during material processing such as the solidification, the electro-deposition and the phase transformation [1]. Owing to the unusual magnetic and magneto-optical properties, the physical properties of the binary compound MnBi have been investigated extensively [2–8]. Effect of a high magnetic field on the microstructure of the MnBi compounds has been investigated. Savitsky et al. [9] and Asai et al. [10,11] found that MnBi phase aligned regularly along the magnetic field in Bi–0.9–10 wt%Mn alloy solidified in the 2.5–5 T magnetic field. However, up to now, little work has been investigated the effect of magnetic field on the morphology of MnBi phase and its magnetic properties of the MnBi compounds. Especially, little work has been investigated the effect of a high magnetic field on the morphology and magnetic properties of the MnBi compounds during the Mn<sub>1.08</sub>Bi–MnBi phase transformation process.

In Ref. [12], the effect of a high magnetic field on the Mn<sub>1.08</sub>Bi–MnBi phase transformation has been investigated. This work extends the work in Ref. [12] and investigates on the effect of a high magnetic field on the morphology and magnetic properties of the MnBi compounds around the Mn<sub>1.08</sub>Bi–MnBi

phase transformation. It has been found that the field has separated the MnBi crystal along the (001)-crystal plane and the split MnBi crystals align and aggregate along the magnetic field direction during the Mn<sub>1.08</sub>Bi–MnBi phase transformation process. Along with the change of the MnBi phase morphology, the magnetic property has changed greatly. Indeed, with the alignment and aggregation of the split MnBi phases, the saturation magnetization  $M_s$  and the magnetic susceptibility  $\chi$  increase, and the coercive field  $H_c$  and the remnant magnetization  $M_r$  decrease. This implies that the field may have caused the magnetic property of the MnBi phase to transform towards soft magnetism.

## 2. Description of the experiments

Bi–6 wt%Mn alloys were prepared using bismuth (99.999% purity) and electrolytic manganese (99.5%). Raw materials were melted in an induction furnace and cast to a graphite mold under argon at a pressure of 50.6 kPa. The samples with 9.5 mm diameter and 25 mm length were sealed in a graphite tube and inserted into a resistance furnace placed into the magnet. The intensity of the magnetic field (up to 14 T) could be adjusted and the temperature in the furnace chamber could be controlled automatically during the experiment as shown in Fig. 1. The temperature in the furnace could reach 1000 °C, and was measured with the precision of  $\pm 1$  K by a NiCr–NiSi thermocouple which was in direct contact with the sample.

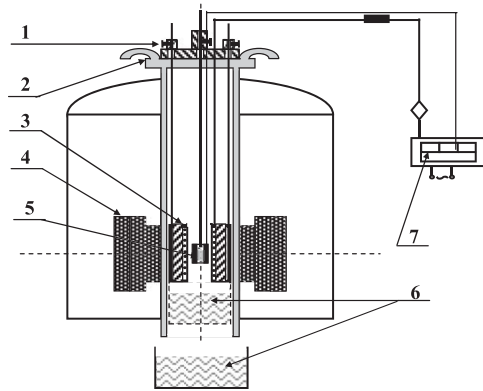
The samples were solidified under various solidification conditions and the magnetic field was imposed at a certain stage

\* Corresponding author at: Department of Material Science and Engineering, Shanghai University, Shanghai 200072, PR China.  
E-mail address: [xi@hmg.inpg.fr](mailto:xi@hmg.inpg.fr) (X. Li).

during the solidification process. The samples obtained in the above experiments were sectioned along the direction parallel and perpendicular to the applied magnetic field  $H_f$  during the solidification. The microstructures on both longitudinal and transverse sections of the samples were polished mechanically and characterized by the optical microscopy. Magnetic measurements were conducted under the applied magnetic field  $H_m$  up to 50 kOe by a physical properties measurement system (PPMS/Quantum Design). Samples were cut in the shape of cubes (to avoid demagnetization factor consideration) with the edges parallel and perpendicular to the  $H_f$  direction.

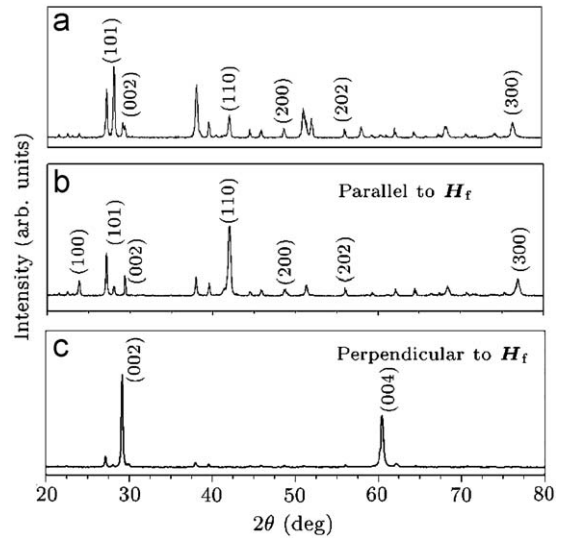
### 3. Results

Fig. 2 shows the microstructures heated to a certain temperature and held for 30 min, and then solidified at a



**Fig. 1.** Schematic diagram of the experimental device of metal solidification in high magnetic field: (1) Sample frame, (2) water-cool cover, (3) heating furnace, (4) superconductor magnet, (5) sample, (6) quenching water-pond and (7) controlling temperature system.

cooling rate of 10 K/min below 262 °C (eutectic point temperature) under a 10 T magnetic field. Fig. 2(a) and (b) show transverse and longitudinal microstructures of the sample solidified from 350 °C, respectively. It can be observed that the elongated MnBi phases (dark gray) are oriented with a longer axis along the magnetic field direction in the Bi matrix (white). The hexagonal profile of the crystals only appears in the section perpendicular to the magnetic field. This should be attributed to the magnetic crystalline anisotropy of the MnBi crystal and the alignment of the MnBi phase under a high magnetic field [9–11]. Fig. 2(c) and (d) show the transverse and longitudinal microstructures of sample



**Fig. 3.** XRD patterns of the sample solidified from 360 °C in Fig. 2: (a) 0 T, (b) section parallel to  $H_f$  and (c) section perpendicular to  $H_f$ . Peaks labeled by (hkl) are for MnBi and others for Bi.

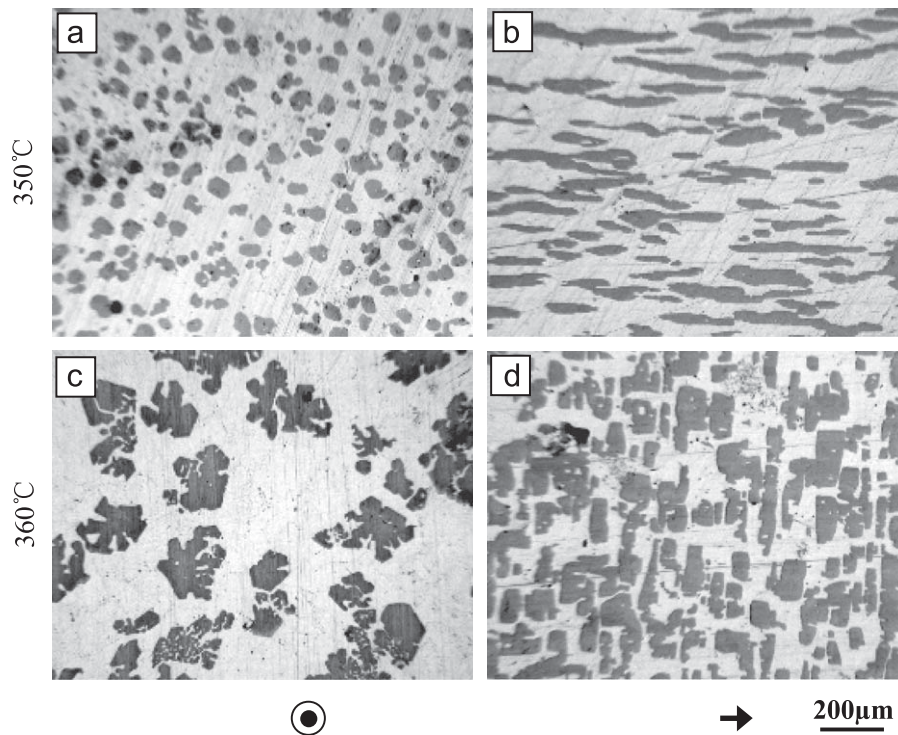


**Fig. 2.** Microstructures solidified from a certain temperature at a rate of 10 K/min after holding temperature for 30 min at this temperature under a 10 T magnetic field.

solidified from 360 °C, respectively. Compared with the microstructure solidified from 350 °C, it can be observed that the morphology of the MnBi phase has been changed significantly. Indeed, it can be observed that MnBi crystals are separated along the section perpendicular to the  $H_f$  direction and oriented with a

shorter axis along the  $H_f$  direction. Furthermore, the XRD patterns (Fig. 3) show that the  $\langle 001 \rangle$ -crystal direction (i.e., the easy magnetization axis) of the MnBi crystal is aligned along the magnetic field direction. This means that the MnBi crystal in the sample solidified from 360 °C is separated along the  $(001)$ -crystal

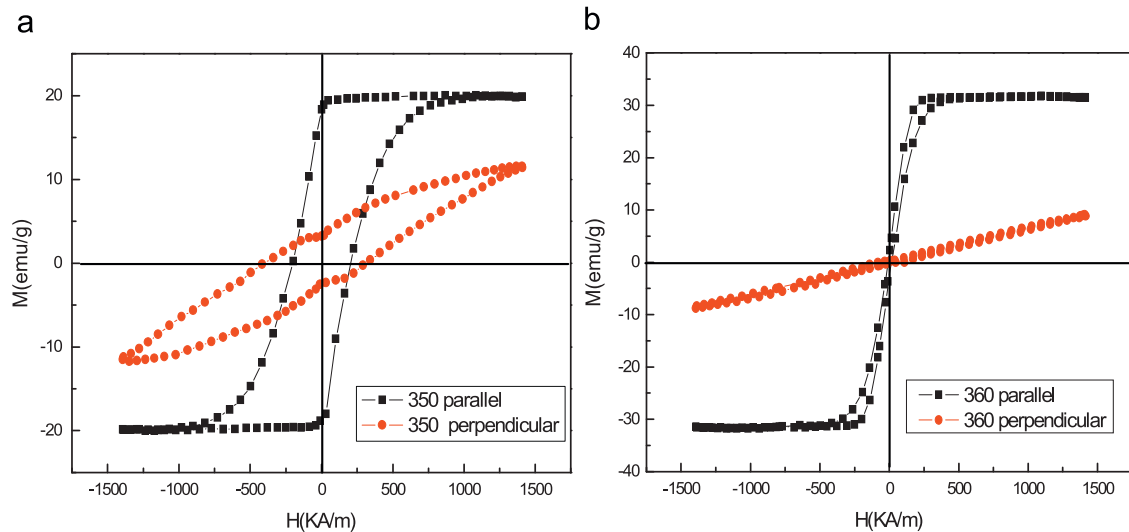


**Fig. 4.** Hysteresis loops of the same samples as shown in Fig. 2. (a) 350 °C and (b) 360 °C. “Parallel and perpendicular” indicate directions of the magnetic field imposed for the magnetization measurement ( $H_m$ ) with respect to the magnetic field imposed during the solidification ( $H_f$ ).

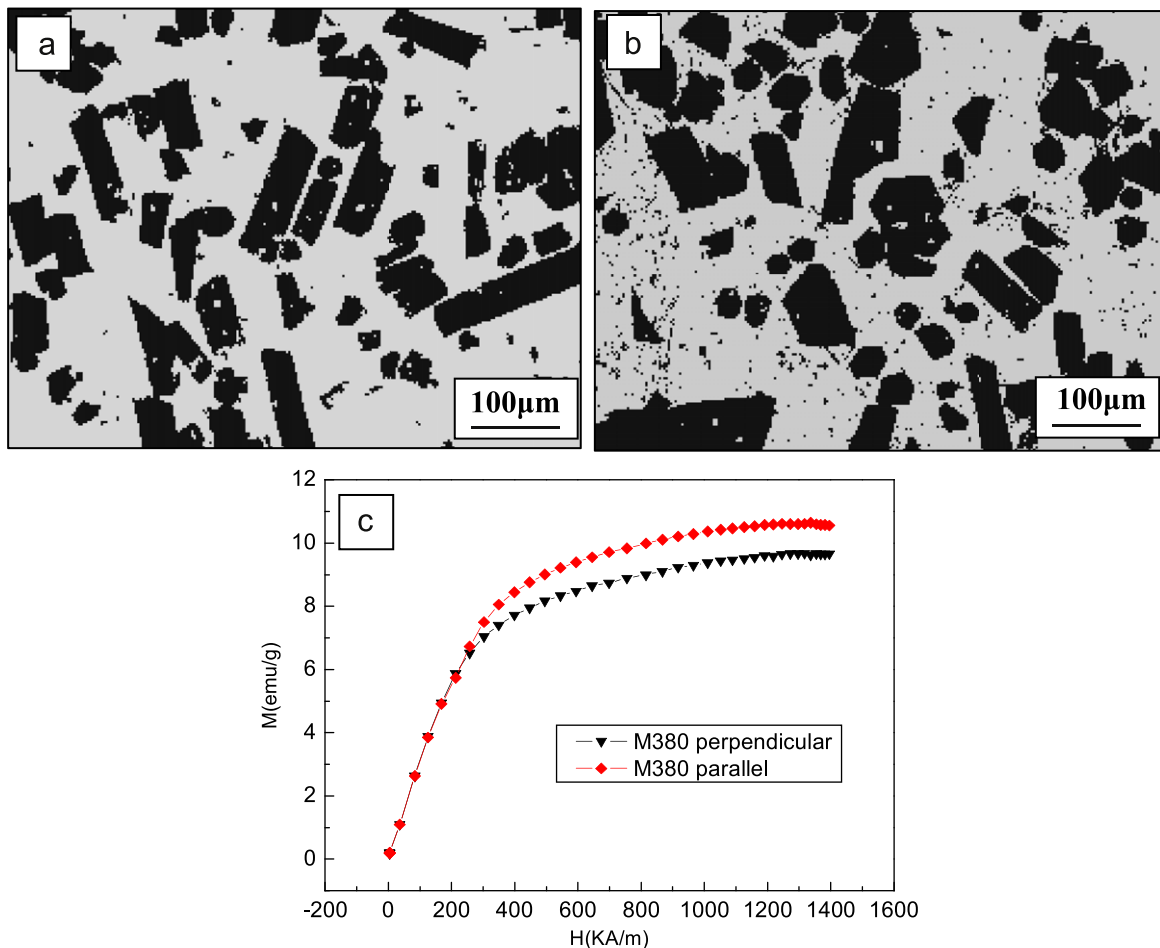


**Fig. 5.** Microstructures and magnetization curves for the sample solidified from 400 °C at a rate of 10 K/min to 380 °C after being holding temperature for 30 min with a 10 T magnetic field, and then quenched: (a) longitudinal section, (b) transverse section and (c) magnetization curves.

plane. To investigate the magnetic property, the hysteresis loops of samples have been measured. Because Bi is diamagnetic, its effect has been ignored and only the MnBi compounds have been considered in the magnetization measurement. Fig. 4 shows the hysteresis loops parallel and perpendicular to the  $H_f$  direction for the samples referred in Fig. 2. It can be learned that the coercive field  $H_c$  and the remnant magnetization  $M_r$  of the sample solidified from 360 °C are much lower than the one of the samples solidified from 350 °C. However, its saturation magnetization  $M_s$  is larger than the one of the samples solidified from 350 °C.

From the phase diagram of the Mn–Bi alloy [13], it can be learned that the paramagnetic  $Mn_{1.08}Bi$  compound is formed by the peritectic reaction of  $Mn+L(Bi) \rightarrow Mn_{1.08}Bi$  at 446 °C; furthermore, the compound undergoes a magnetic and structure transformation to form ferromagnetic MnBi phase at 340 °C upon cooling, and MnBi phase turns into the  $Mn_{1.08}Bi$  at 355 °C upon heating. The MnBi phase is called as low-temperature phase (LTP), the  $Mn_{1.08}Bi$  is called as high-temperature phase (HTP) and the quenched state of HTP is called as the quenched high-temperature phase (QHTP). Therefore, when the sample is solidified from 360 °C, the MnBi phase is formed during the  $Mn_{1.08}Bi$ –MnBi phase

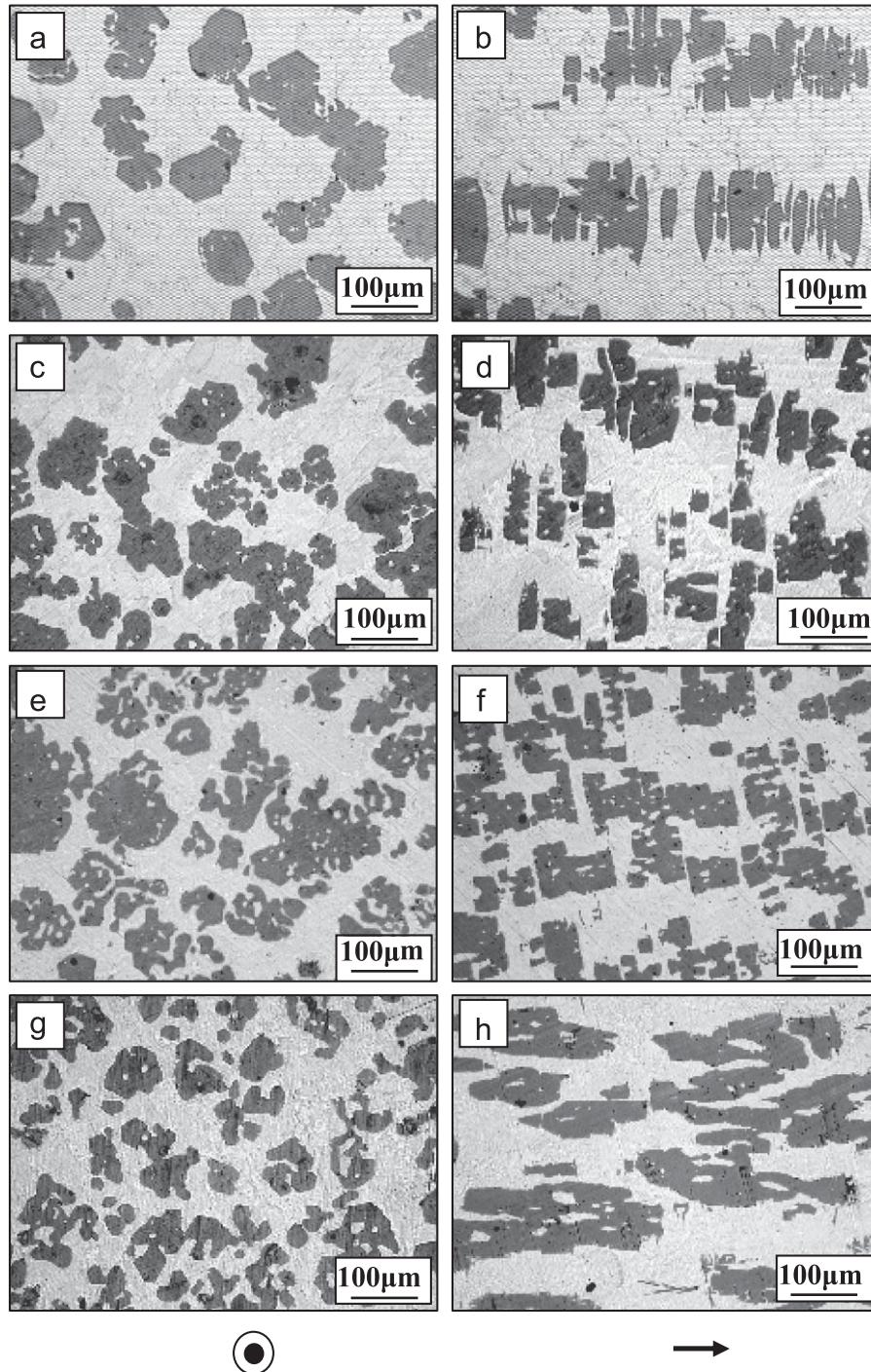


**Fig. 6.** Microstructures of the Bi–6wt%Mn alloy cooled from 400 to 360 °C and held for 5 min (a, b), 10 min (c, d), 30 min (e, f) and 60 min (g, h) and then quenched in a 10 T magnetic field, respectively.

transformation process. The above results imply that a high magnetic field has changed the microstructure and magnetic properties of the MnBi phase during the Mn<sub>1.08</sub>Bi–MnBi phase transformation process.

Moreover, the effect of a high magnetic field on the morphology and magnetic properties of the paramagnetic Mn<sub>1.08</sub>Bi phase has also been investigated. Fig. 5 shows the microstructures of the samples solidified from 400 °C at a cooling rate 10K/min and quenched at 380 °C. It can be observed that there are no clear influences of the field on the morphology of the primary Mn<sub>1.08</sub>Bi phase. This means that a 10T magnetic field cannot align the paramagnetic Mn<sub>1.08</sub>Bi phase. Further, the magnetization of the sample was measured and Fig. 6 presents the magnetizations parallel and perpendicular to the  $H_f$  direction for samples in Fig. 5. It can be observed that there is no obvious magnetic anisotropy. This is consistent with the alignment behaviours of the paramagnetic Mn<sub>1.08</sub>Bi phases under the magnetic field. This shows that an application of a 10T high magnetic field has few influences on the paramagnetic Mn<sub>1.08</sub>Bi phase. Therefore, the change of the morphology and magnetic property of the sample under a high magnetic field should be attributed to the effect of the magnetic field on the MnBi phase.

Further, the effect of the holding temperature times at 360 °C under a 10T magnetic field on the morphology and magnetic property of the MnBi compounds has been investigated. Fig. 6 shows the microstructures solidified from 400 °C and held various times at 360 °C before quenching. It can be observed that with the increase of the holding temperature time under the magnetic field, the phase is separated gradually along the plane perpendicular to the magnetic field, and the split phases align and aggregate along the magnetic field direction. Fig. 7 shows the magnetizations (Fig. 7(a)) and hysteresis loops (Fig. 7(b)) for the samples as referred in Fig. 6. It can be observed that with the increase of the holding temperature time under the magnetic field, the saturation magnetization  $M_s$  and the magnetic susceptibility  $\chi$  increase. The remnant magnetization  $M_r$  and the ratio of  $M_r/M_s$  (Fig. 7(c)) decrease. The above results indicate that the morphology and the magnetic properties ( $M_r$  and  $M_r/M_s$ ) of the MnBi compounds have changed significantly with the increase of the holding temperature time under a high magnetic field.

#### 4. Discussion

Above experimental results have shown that the morphology and the magnetic property of the MnBi compounds have been changed significantly during the Mn<sub>1.08</sub>Bi–MnBi phase transformation process under a high magnetic field. This should be attributed to the enhancement of a high magnetic field on the magnetization of the MnBi phase and the Mn<sub>1.08</sub>Bi–MnBi phase transformation.

As shown in Fig. 8(a), the ferromagnetic MnBi phase (LTP) will nucleate on the surface of the paramagnetic Mn<sub>1.08</sub>Bi phase (HTP) during the Mn<sub>1.08</sub>Bi–MnBi phase transformation process. Along with the formation of the MnBi phase, the magnetic domains will produce. When the magnetic field is applied, the MnBi phase will be magnetized; as a consequence, the magnetic domains will rotate and the magnetic domain walls will move. Thus, their same-name magnetic poles will align along the magnetic field direction (Fig. 8(b)) and then repulsive forces will produce among them. The repulsive force can be expressed as [14]:

$$F_M = \frac{\mu_0(\chi + 1)}{4\pi} \frac{Q_{m1}Q_{m2}}{r^2} \quad (1)$$

where  $Q_{m1}$ ,  $Q_{m2}$  are the strength of two magnetic poles,  $r$  the distance between two magnetic poles. With the growth of the LTP

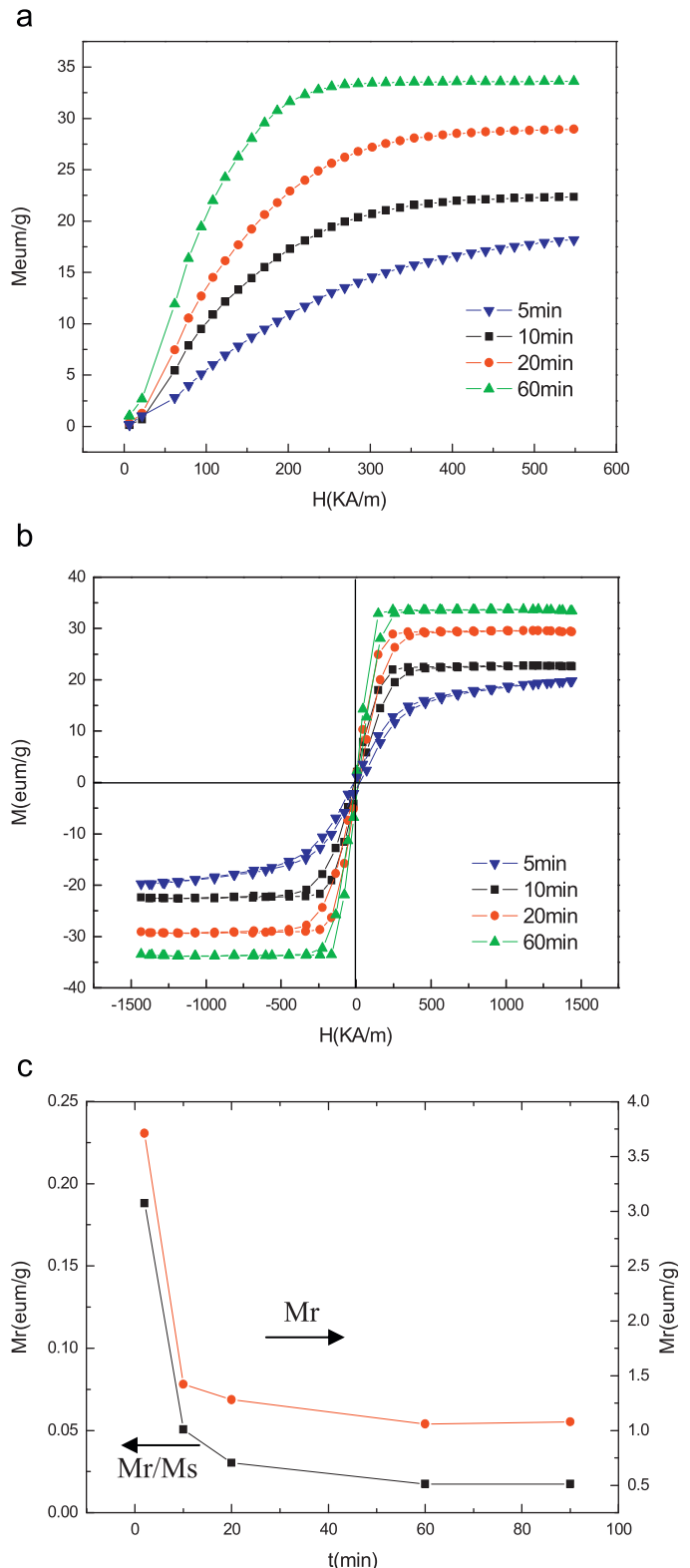


Fig. 7. The magnetic properties of the same sample as shown in Fig. 6. (a) Magnetizations, (b) hysteresis loops, (c) remnant magnetization  $M_r$  and the  $M_r/M_s$ . The directions of the magnetic field imposed for the magnetization measurement ( $H_m$ ) is parallel to the magnetic field imposed during the solidification ( $H_f$ ).

phase, their volumes increase and the inter-grains distances decrease. Thus, according to the formula (1), the repulsive forces increase significantly. Consequently, the force will separate the

MnBi grains. At the same time, the split MnBi crystals will align and aggregate along the magnetic field direction as shown in Fig. 8(c). Thus, the microstructures in Figs. 2 and 6 will form.

Moreover, from the magnetism point of view, the magnetic domains in the substance rotate their easy magnetic axes towards the magnetic field direction by moving their magnetic domain walls during the magnetization process. The grain boundary stress will retard the rotation and movement of the domains. Thus, the large coercive field  $H_C$  and the remnant magnetization  $M_r$  will

form. It is well known that the LTP (MnBi phase) has the large coercive field  $H_C$  and the remnant magnetization  $M_r$ . During the  $Mn_{1.08}Bi$ -MnBi phase transformation under a high magnetic field, the magnetic domain walls may be destroyed. Thus, the stresses in the grains are released and the magnetostriction is reduced; which will lead to the reduction of the coercive field  $H_C$  and the remnant magnetization  $M_r$  in the MnBi phase. Furthermore, the reduction of the magnetic domain walls and magnetostriction causes the motion of the magnetic domain to be easier. As a result, its magnetic susceptibility  $\chi$  will increase. It has been reported that the cracks occurred frequently during the directional solidification of the TbDyFe alloy under a high magnetic field [15]. This may be attributed to the same mechanism presented here. As they both endure the peritectic transformation during the solidification process. From this mechanism, it may be concluded that the application of a high magnetic field during the peritectic phase transformation involving of a ferromagnetic phase will result in the increase of the magnetic susceptibility  $\chi$  and the decrease of the coercive field  $H_C$  and the remnant magnetization  $M_r$ .

As the MnBi crystal has owned a larger saturation magnetization  $M_s$ , the increase of the saturation magnetization  $M_s$  during the  $Mn_{1.08}Bi$ -MnBi phase transformation process in a high magnetic field may be attributed to the increase of the MnBi phase. There are several reasons; first, owing to the decrease of the MnBi free energy under the magnetic field, the  $Mn_{1.08}Bi$ -MnBi phase transformation course will be enhanced. Consequently, the content of the MnBi phase increases. Second, owing to the increase of the  $T_C$  under the magnetic field [12] the equilibrium liquidus near MnBi may be elevated. If ignoring the influence of the field on the melting point of Bi (because it is diamagnetic) and liquidus near it, the application of the magnetic field will cause an increase of eutectic temperature and a shift leftward of the eutectic composition as shown in Fig. 9(b). Thus, the content of the MnBi phase in the alloy will increase. Moreover, the separation of the MnBi phase also enhances the  $Mn_{1.08}Bi$ -MnBi phase transformation process and leads to the increases of the MnBi phase. Moreover, the above experimental results have shown that with the increase of the holding temperature time, the saturation magnetization  $M_s$  will increase. This should be attributed that with the increase of the holding temperature time, the  $Mn_{1.08}Bi$ -MnBi phase transformation has been enhanced. Thus, the content of the MnBi phase increases. Since the MnBi crystal has owned a large saturation magnetization  $M_s$ , the saturation magnetization  $M_s$  of the sample will increase.

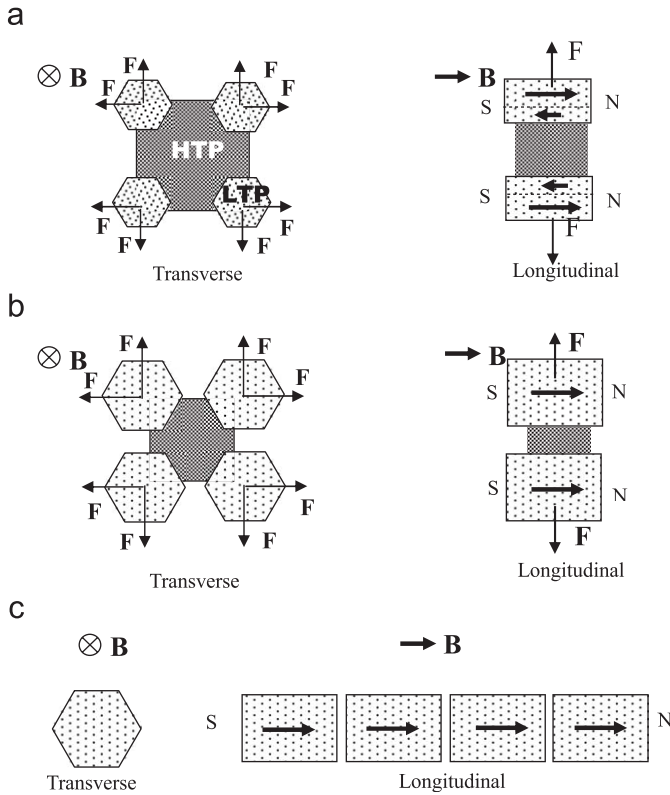


**Fig. 8.** Schematic illustration of the  $Mn_{1.08}Bi$ -MnBi phase transformation process in the magnetic field: (a) generation of magnetizing forces between the ferromagnetic MnBi phases (LTP) in the magnetic field, (b) the increase of the magnetizing forces along with the growing up of the MnBi phase and (c) aggregation of the MnBi phases.

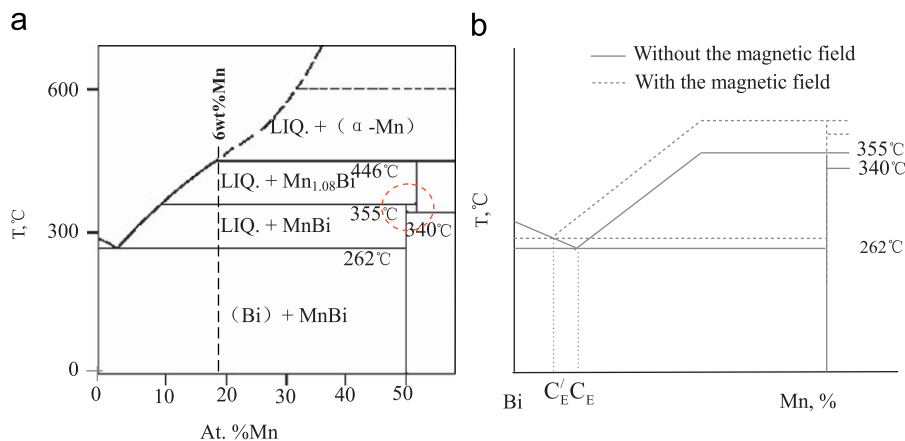


**Fig. 9.** Effect of the magnetic field on the equilibrium phase diagram of Mn-Bi system: (a) equilibrium phase diagram of Mn-Bi system near Bi, red circle showing the  $Mn_{1.08}Bi$ -MnBi phase transformation and (b) schematic illustration of the modification of the phase diagram by the magnetic field.

## 5. Conclusions

Effect of a high magnetic field on the morphology and magnetic properties of the MnBi compounds during the Mn<sub>1.08</sub>Bi–MnBi phase transformation process has been investigated. Results indicate that the field has separated the MnBi crystal along the (001)-plane during the Mn<sub>1.08</sub>Bi–MnBi phase transformation process and the split MnBi crystals align and aggregate along the magnetic field direction. Along with the change of the morphology of the MnBi compounds, the magnetic properties of the MnBi phase has been changed significantly; as a result, the saturation magnetization  $M_s$  and the magnetic susceptibility  $\chi$  increase, and the coercive field  $H_c$  and the remnant magnetization  $M_r$  decrease. This should be attributed to the transformation of the magnetic property of the MnBi phase towards soft magnetism during the Mn<sub>1.08</sub>Bi–MnBi phase transformation under a high magnetic field and the enhancement of a high magnetic field on the magnetization of the MnBi phase and the Mn<sub>1.08</sub>Bi–MnBi phase transformation.

## Acknowledgments

This work is supported partly by the European Space Agency through the IMPRESS project, Natural Science Foundation of China

(No. 50801045) and the Changjiang Scholars and Innovative Research Team in University (No: IRT0739).

## References

- [1] S. Asai, Sci. Technol. Adv. Mater. 1 (2000) 191 (and its references).
- [2] J.B. Yang, K. Kamaraju, W.B. Yelon, W.J. Jame, Appl. Phys. Lett. 79 (2001) 1846.
- [3] Y.Q. Xu, B.C. Liu, D.G. Pettifor, Phys. Rev. B 66 (2002) 184435.
- [4] J.B. Yang, W.B. Yelon, W.J. James, Q. Cai, M. Kornecki, S. Roy, N. Ali, J. Phys.: Condens. Matter 14 (2002) 6509.
- [5] T. Hihara, S.Y. Koi, J. Phys. Soc. Jpn. 29 (1970) 343.
- [6] T. Chen, W. Stutius, IEEE Trans. Magn. 10 (1974) 581.
- [7] S. Saha, R.T. Obermyer, B.J. Zande, V.K. Chandhok, S. Simizu, S.G. Sankar, J.A. Horton, J. Appl. Phys. 91 (2002) 8525.
- [8] K.U. Harder, D. Menzel, T. Widmer, J. Schoenes, J. Appl. Phys. 84 (1998) 3625.
- [9] E.M. Savitskiy, R.S. Torchinova, S.A. Turanov, J. Cryst. Growth 52 (1981) 519.
- [10] K. Sassa, H. Yamao, S. Asai, in: M. Garnier (Ed.), Proceedings of the International Symposium on Electromagnetic Processing of Materials, Paris, July 1997, 157.
- [11] H. Morikawa, K. Sassa, S. Asai, Mater. Trans. JIM 39 (1998) 814.
- [12] X. Li, Z.M. Ren, Y. Fautrelle, Mater. Lett. 60 (2006) 3379.
- [13] W.G. Moffatt, in: The Handbook of Binary Phase Diagrams, Genium, USA, 1984, p. 11.
- [14] E. Hallen, Electromagnetic Theory, Chapman & Hall Ltd, London, 1962, p. 185.
- [15] H. Minagawa, et al., J. Magn. Mater. 248 (2002) 230.